ITEP-22-94

Fermilab Library
0 1160 0037132 2

INSTITUTE OF THEORETICAL
AND EXPERIMENTAL PHYSICS

ITEP-22-94

22

L.G.Vorobiev

Two-dimensional particle code for beam simulation in HIF driver

FERMILAB
JUN 28 1994
LIBRARY

MOSCOW 1994

UDK 621.384.663:517 M-16

TWO-DIMENSIONAL PARTICLE CODE FOR BEAM SIMULATION IN HIF DRIVER; Preprint ITEP 22-94/

L.G.Vorobiev - M., 1994 - 24p.

A particle code has been devised for high-current beam simulation in a driver for heavy ion fusion (HIF). Some suggestions have been offered for efficient implementation of the algorithm. To illustrate it's applications a final focusing system of HIF driver has been designed and a numerical simulations of beam focusing onto the thermonuclear pellet has been carried out. An advanced "charge-symmetrical" driver's scheme has been also considered and some comparisions with conventional schemes have been made.

Fig. - 12, ref. - 18

© Институт теоретической и экспериментальной физики, 1994

1 Introduction

An accelerator driver for heavy ion fusion (HIF), which operates with very intense high energy ion beams, will represent in all respects a state-of-the-art facility. Due to a very high cost of the driver (see [1]-[4]), a detailed large-scale numerical simulations play a very important role in preliminary studies. So far as a detailed analytical self-consistent analysis of beam motion is available only in frames of simplest models (for beams with 1 degree of freedom, e.g. for 1D sheet beam, etc.) the only practical approaches for accurate description of intense beams are the so-called envelope or K-V equations [5], and numerical simulation, using particle codes.

The special features of two-dimensional K-V beams have been discussed in detail earlier (see papers [5,6,7]). This 2D model presents fairly a good accuracy for intense beam behavior, when the major contributions of space charge forces (linear terms) are taken into account. K-V model is also convenient for fitting procedures, because the fast computing of beam parameters gives the opportunity to search for the best variants automatically – to optimize the focusing lattice and to design various optical insertions for high-current beams handling. The limitations of K-V equation are, that they are valid only in the absence of nonlinearities and when the rms emittance is constant. Meantime, just these phenomena take place in HIF driver and become decisive factors especially at the driver's final stage – within final focusing objective. All that necessitates to use two- and three-dimensional particle codes.

In the proposed paper a 2D particle code will be described and it's applications will be illustrated by beam dynamics simulation in HIF driver. Some computational blocks, which could be helpful for algorithm implementation, will be discussed as well.

2 Two-dimensional particle code

Numerical simulation using super-particles, represents an universal tool of computational physics and has a number of applications (see Hockney's book [8]). Despite of these applications diversity, the most of algorithms include, as usual, the following computational blocks:

1. An algorithm for initial ions coordinates and velocities arrangement,
2. Calculation of space-charge forces,
3. Numerical integration of beam motion equations,

where second and third steps are being performed in cycle.

A computer program, outlined below, follows this general scheme. At the same time, when designing HIF final focusing system, it has appeared to make serious efforts, in order to upgrade the computational characteristics of the algorithm in terms of the integration method accuracy and the rapidness of the calculations. A simple numerical procedure to find a family of rms-matched beams (initial distribution) has been also developed.

2.1 Algorithm for initial distribution

As is well known, for periodical focusing channel, only microcanonical distribution function allows to find exactly the integral of motion, which is represented by Hamiltonian H ($dH/dt \equiv 0$). It was found in [5], that $f(H) = \delta(H - H_{max})$, i.e. all particles belongs to the ellipsoidal shell in the four dimensional phase space (x, p_x, y, p_y), all phase-density projections are elliptical, uniform ($\varrho = const$), and the corresponding space charge forces are linear. Assuming, that the beam has a crossover ($g'_x = 0$, where g stands for the beam envelopes) in the initial point, the corresponding Hamiltonian H may be written as the following:

$$H = \frac{x^2}{a_x^2} + \frac{{p_x}^2}{a_{p_x}^2} + \frac{y^2}{a_y^2} + \frac{{p_y}^2}{a_{p_y}^2} \tag{1}$$

The numerical procedure to arrange a K-V phase distribution is assumed to be well known and we do not consider it.

Meantime, real beams have smooth phase and space charge densities. In the papers [7] it was proven, that assuming the rms emittance is constant, the corresponding rms envelope equations are valid for K-V beam ($\rho = const$), as well as for any other beam with $\varrho(r) \neq const$. When beam propagates through the long periodical focusing channel and rms emittance growth is not significant, the above proposition seems to be quite justified. We shall devise therefore an algorithm, which forms a class of rms-matched distributions, those which provide the coincidence of different momenta of $f(H)$ with the K-V distribution.

Thus, the Hamiltonian H is assumed to be an integral of motion for a family of phase distributions with distribution function $f(H) = (1 - H/H_{max})^{s-1}$ and real space density $\varrho(r) = \varrho_0(s)(1 - r^2/r_m^2)^s$ (see figs.1a – 1b), where H varies within $H \in [0, H_{max}]$, r_m is a beam size, and $s > 0$. (One can see, that the singular K-V distribution can be obtained, when taking $s = 0$).

If the distribution function $f(H)$ in the phase space is known, then the particles number within the elementary volume $dV(H)$ can be found from the formula

$$dN(H) = f(H)dV(H) \tag{2}$$

A general expression for dV can be written as:

$$dV(H) = dx dp_x dy dp_y \tag{3}$$

If Hamiltonian is expressed by the formula (1), and $R = a_x = a_y$, $P = a_{x'} = a_{y'}$ (circular beam), then, introducing the cylindrical coordinates, we can rewrite $H = r^2/R^2 + p^2/P^2$ and $dV(H) = r dr d\phi_r p dp d\phi_p$. After integrating, one can obtain the dependence $V(H)$, as

$$V(H) = \int r dr d\phi_r p dp d\phi_p = \pi^2 \int_0^{r^2(H)} \int_0^{p^2(H)} dr^2 dp^2 \tag{4}$$

Since $r^2(H) = HR^2$ and $p^2(H) = P^2(H - r^2/R^2)$, one gets

$$V(H) \propto \pi^2 P^2 \int_0^{HR^2} (H - r^2/R^2) dr^2 = \frac{1}{2}\pi^2 P^2 R^2 H^2 \tag{5}$$

Hence, the Eq.(2) can be written as

$$dN(H) \propto f(H) H dH$$

If we consider now a discrete distribution $\{H_i\}$ ($H_i = H_{i-1} + dH_i$), then instead of above differential relation we have

$$dN(H_i) = dN_i = C_1 f(H_i) H_i dH_i$$

The derived formula expresses the dependence of particles number from Hamiltonian. If we now demand the performance of

$$S_i = f(\widetilde{H_i}) H_i dH_i \equiv const \qquad i = 1, 2, \ldots, M \tag{6}$$

(where $H_{i-1} \leq \widetilde{H_i} \leq H_i$ and $dH_i = H_i - H_{i-1}$), then we can form an arbitrary bivariate distribution, as a superposition of K-V distribution components with $f(H_i)$, if only a discrete set $\{H_1, H_2, \ldots, H_M\}$, will satisfy the conditions (6) (see fig.1c). The particles numbers in every layer, must be constant, whereas the

dH_i varies: $dH_i \neq dH_{i+1}$. A possible way to find the corresponding distribution $\{H_i\}$, is proposed in Appendix 1.

(Note, that the alternative way to assign the distribution is to arrange a superposition of singular K-V distributions on the regular set $\{H_i\}$ with $dH_i = const$. However, in this case, we have to vary the number of particles within every K-V layer. For big enough number of particles, the both approaches, certainly, coincide.)

Hence, the semiaxes of ellipses (the components, having K-V distributions) can be found as the following:

$$a_{ix} = a_{mx}\sqrt{h_i} \qquad a_{iy} = a_{my}\sqrt{h_i} \qquad a'_{ix} = a'_{mx}\sqrt{h_i} \qquad a'_{iy} = a'_{my}\sqrt{h_i}$$

where $h_i = H_i/H_{max}$, $i = 1, \ldots, M$ and a_{mx}, a_{my} are maximal beam's sizes. As long as the rms beam sizes must coincide, one can derive, that

$$r_0^2 = < r^2 > = \frac{\int f(H) r^3 dr d\phi_r \cdot p dp d\phi_p}{\int f(H) r dr d\phi_r \cdot p dp d\phi_p} = \frac{\int \varrho(r) r^3 dr}{\int \varrho(r) r dr} = \frac{r_m^2}{p+2}$$

that determines the magnitudes of a_{mx}, a_{my}.

Thus, the above described technique, give a simple algorithm to arrange a class of rms-matched initial distributions (see [9]).

2.2 Space-charge forces calculations

There are two ways to find space charge forces. The first way is to compute all couple forces between all superparticles in the assembly – PP (particle-particle) model. It is clear, that the number of operations required is of the order $O(N_p^2)$ in every step and is very time-consumed.

Another more cheaper computational approach is to find these forces by solving the Poisson equation over a bivariate region R with Dirichlet and Neumann boundary conditions

$$\begin{cases} \nabla^2 u = -\rho(x_1, x_2), \qquad (x_1, x_2) \in R, \qquad \text{subject to:} \\ u(x_1, x_2)|_\Gamma = 0 \\ \dfrac{\partial u(x_1, x_2)}{\partial n} = 0|_\gamma = 0 \end{cases} \tag{7}$$

where Γ and γ define the boundaries of the R region.

According to this approach, the differential problem is replaced by a discrete one, by introducing a spatial discrete grid (PM-approach, "particle-mesh"). A number of various algorithms exist now to solve discrete Poisson equation for a wide enough range of regions. (We should remind about the more advanced combined PP-PM, or P^3M method, which is described in [8], but we use in the particle code PM approach, which presents a sufficient efficiency). Those which

are based on Fast Fourier Transformation (FFT) provide, apparently, the most economical methods in terms of the total computer operations count.

The algorithm, described in the paper [11], is applied for the simplest circle and rectangular regions with symmetrical boundary conditions (the particle code uses only rectangular grid to provide a simple compatibility with density block). Namely, the algorithm operates, in the following regions (see figs.2a –2c)

$$R_1 = \{(x_1, x_2) : -d_1 < x_1 < d_1, -d_2 < x_2 < d_2\}$$
$$R_2 = \{(x_1, x_2) : -d_1 < x_1 < d_1, \ -d_2 < x_2 < 0\}$$
$$R_3 = \{(x_1, x_2) : -d_1 < x_1 < 0, \ \ -d_2 < x_2 < 0\}$$

The algorithm is based on Fourier decomposition in one dimension, using FFT technique, and solve a series of tridiagonal systems in the second dimension [11].

According to PM-approach, the $\varrho(x_i, y_j)$ function is being determined at the grid points by a special redistribution scheme: the particle's charge is being assigned proportionally to the shape factor of the particle's cloud. The following options of superparticle shape-functions are available in the particle code:

$$\begin{cases} S_1(x') = \frac{1}{2\Delta} & S_2(x') = \frac{3}{4\Delta}(1 - \frac{x'^2}{\Delta^2}) \\ S_3(x') = \frac{1}{2\Delta}(1 + \cos(\frac{\pi x'}{\Delta})) & S_4(x') = \frac{1}{3\Delta}(1 + \cos(\frac{\pi x'}{\Delta}))^2 \\ S_5(x') = \frac{15}{16\Delta}(1 - \frac{x'^2}{\Delta^2})^2 & \end{cases} \tag{8}$$

and in fig.3a one-dimensional slices of the clouds are plotted (naturally, the particle clouds themselves are two-dimensional).

The corresponding $\Phi(x, a) = \int_a^x S(x')dx'$ (see fig.3b) are the following

$$\begin{cases} \Phi_1(x, a) = \frac{x - a}{2\Delta} & \Phi_2(x, a) = \frac{3(x - a)}{4\Delta} - \frac{x^3 - a^3}{4\Delta^3} \\ \Phi_3(x, a) = \frac{x - a}{2\Delta} + (\sin\frac{\pi x}{\Delta} - \sin\frac{\pi a}{\Delta})/2\pi & \\ \Phi_4(x, a) = \frac{x - a}{2\Delta} + \frac{1}{12\pi}\left\{8(\sin\frac{\pi x}{\Delta} - \sin\frac{\pi a}{\Delta}) + \sin\frac{2\pi x}{\Delta} - \sin\frac{2\pi a}{\Delta}\right\} & \\ \Phi_5(x, a) = \frac{15(x - a)}{16\Delta} - \frac{5(x^3 - a^3)}{8\Delta^3} + \frac{3(x^5 - a^5)}{16\Delta^5} & \end{cases} \tag{9}$$

In the figs.4a – 4b an uniform density is shown, which has been obtained by means of various algorithms.

The criterion to make a right choice of superparticles sizes and the shape of the cloud is to reduce nonphysical effects due to spatial grid, the finite size of the superparticles, etc. Usually, a series of test simulations should be carried out before the large-scale simulations, to choose the appropriate parameters.

2.3 Numerical integration of motion equations

The equations of ion's motion can be written, as

$$\mathbf{x}''(z) = \frac{1}{\gamma M v^2}\{\mathcal{F}^{ext}(\mathbf{x},z) + \frac{q}{\gamma^2}\mathcal{E}^{sp}(\mathbf{x},z)\} = \mathbf{F}^{ext}(\mathbf{x},z) + \mathbf{F}^{sp}(\mathbf{x},z) \qquad (10)$$

where vector $\mathbf{x} = (x_1, x_2)$ denotes the transversal coordinates and z is the longitudinal coordinate of the ion; vector $\mathcal{F}^{ext} = q[\vec{v}, \vec{\mathbf{B}}]$ stands for external magnetic focusing and vector $\vec{\mathbf{B}}$ denotes the external magnetic field, vector $\mathcal{E}^{sp} = (-\partial u(\mathbf{x},z)/\partial x_1, -\partial u(\mathbf{x},z)/\partial x_2)$ is a strength of space charge electrical field, with the ($u(\mathbf{x},z)$ potential from (7)), M is ion mass, $v = dz/dt$ and γ is relativistic factor. We shall use below the notation $\mathbf{F}(\mathbf{x}) = \mathbf{F}^{ext}(\mathbf{x},z) + \mathbf{F}^{sp}(\mathbf{x},z)$ for the right-hand side of Eq.(10).

The Runge-Kutta fourth order method presents a very effective tool to integrate the motion equation. However it is acceptable for those cases, when the $\mathbf{F}(\mathbf{x})$ function can be precisely calculated in $z + \Delta z, z + \Delta z/6, z + \Delta z/3$. As long as the $F^{sp}(z)$ is define by the actual ion's distribution (a self-consistency of the model), the Runge-Kutta algorithm can not be applied without a violation this consistency, we have to use therefore for integration multistep algorithms. Then, in frames of multistep integration, there are explicit and implicit schemes. The implicit integration is also superior to the explicit "predictor-corrector" approaches in terms of the stability, though is somewhat time-consumed.

We introduce now (see [12]) an implicit fourth-order multistep algorithm for numerical integration of Eq.(10). The following relations can be derived from the equation (10):

$$\int_{z_k}^{z_{k+1}} \{\mathbf{x}'(\tau) - \mathbf{x}'(\tau_k)\} d\tau = \int_{z_k}^{z_{k+1}} \int_{z_k}^{z} \mathbf{F}(\mathbf{x}(\xi),\xi) d\xi d\tau$$

$$\int_{z_{k-1}}^{z_k} \{\mathbf{x}'(\tau) - \mathbf{x}'(\tau_k)\} d\tau = \int_{z_{k-1}}^{z_k} \int_{z_k}^{z} \mathbf{F}(\mathbf{x}(\xi),\xi) d\xi d\tau$$

Subtracting the second equation from the first, we obtain the equivalent expression for original Eq.(10)

$$\mathbf{x}(z_{k+1}) - \mathbf{x}(z_k) - \frac{h_{k+1}}{h_k}\{\mathbf{x}(z_k) - \mathbf{x}_{k-1}\} = \mathcal{I}_2 - \frac{h_{k+1}}{h_k}\mathcal{I}_1 \qquad (11)$$

where the $\mathcal{I}_{1,2}$ notations are

$$\mathcal{I}_1 = \int_{z_{k-1}}^{z_k} \int_{z_k}^{z} \mathbf{F}(\mathbf{x}(\xi),\xi) d\xi dz = \int_{z_{k-1}}^{z_k} (z_{k-1} - z)\mathbf{F}(\mathbf{x}(z),z) dz$$

$$\mathcal{I}_2 = \int_{z_k}^{z_{k+1}} \int_{z_k}^{z} \mathbf{F}(\mathbf{x}(\xi),\xi) d\xi dz = \int_{z_k}^{z_{k+1}} (z_{k-1} - z)\mathbf{F}(\mathbf{x}(z),z) dz$$

The expression (11) is equivalent to the original Eq.(10) and describe the same class of the integration schemes. The next step is to find an approximation for the above integrals $\mathcal{I}_{1,2}$ (see Appendix 2).

After simplification, we obtain

$$\mathbf{x}_{k+1} - (1 + H_k)\mathbf{x}_k + H_k\mathbf{x}_{k-1} = I_2 - H_k I_1 = \sum_{i=k-1}^{k+1} S_k \mathbf{F}_k \qquad (12)$$

where $H_k = h_{k+1}/h_k$, $h_k = z_k - z_{k-1}$ and S_k coefficients are the following

$$\begin{cases} S_{k+1} = \frac{h_k^3}{24\bar{h}_k}(2H_k^2 + H_k^3 - 1) \\ S_{k-1} = \frac{h_{k+1}^3}{24\bar{h}_k}(-H_k + 2/H_k + 1/H_k^2) \\ S_k = \frac{h_k^2}{12}(H_k^3 + 4H_k^2 + 4H_k + 1) \end{cases} \qquad (13)$$

with $\bar{h}_k = (h_{k+1} + h_k)/2$.

The above formulae (12)-(13) represent an implicit integration scheme. The coordinates $\mathbf{x}_{k+1}$ can be found by solving the system of non-linear equations iteratively. When we deal with linear focusing terms, only one iteration is sufficient and a possible "prognosis" $\mathbf{x}_{k+1}^{prog}$ can be found from

$$\mathbf{x}_{k+1} = (1 + H_k)\mathbf{x}_k - H_k\mathbf{x}_{k-1} + S_k\mathbf{F}_k.$$

However, when nonlinear strengths appear, the number of iterations increase up to 2 or 3. Naturally, we should try to reduce this value, and the information about the previous coordinates $\mathbf{x}_k, \mathbf{x}_{k-1}, \mathbf{x}_{k-2}$ and strengths $\mathbf{F}_k, \mathbf{F}_{k-1}, \mathbf{F}_{k-2}$ might be very helpful to find a prognosis $\mathbf{x}_{k+1}^{prog}$ more precisely, that helps to avoid extra iterations.

Up to now, it has been assuming, that $\mathbf{F}(z)$ function is a smooth one and has the smooth derivatives up to $\mathbf{F}^{(4)}(z)$. This assumption is absolutely justified for space charge forces. As regards to the external focusing forces, the situation is not so clear. Naturally, the fringing fields at the focusing elements have a smooth ramp, though, in practice, designers deal with the "effective length", which takes into account the influence of the fringing fields in the whole, and the external force in such a lens is abrupted sharply. We adopt now the integration scheme for the class of the functions F^{ext}

$$\mathbf{F}^{ext} = \begin{cases} G^{-}\varphi(\mathbf{x}, z), & \text{for} \quad z \le z_k \\ G^{+}\varphi(\mathbf{x}, z), & \text{for} \quad z > z_k \end{cases}$$

where $\varphi(\mathbf{x}, z)$ – a smooth function.

As an illustration, for quadrupole lens exit, one obtains:

$$\mathbf{F}_x^{ext} = \begin{cases} G^- x, & \text{for} \quad z \le z_k \\ 0, & \text{for} \quad z > z_k \end{cases}$$

$$\mathbf{F}_y^{ext} = \begin{cases} -G^- y, & \text{for} \quad z \le z_k \\ 0, & \text{for} \quad z > z_k \end{cases}$$

with $G^- = kB/a, G^+ = 0$. It is denoted B is a pole tip magnetic field and a is an aperture radius (k is a scaling factor).

For octupole lens entrance one obtains:

$$\mathbf{F}_x^{ext} = \begin{cases} G^+ x(3y^2 - x^2), & \text{for} \quad z \le z_k \\ 0, & \text{for} \quad z > z_k \end{cases}$$

$$\mathbf{F}_y^{ext} = \begin{cases} -G^+ y(3x^2 - y^2), & \text{for} \quad z \le z_k \\ 0, & \text{for} \quad z > z_k \end{cases}$$

Thus, we should devise an fourth order integration scheme for the following equation

$$\mathbf{x}''(z) = \mathbf{F}^{ext}(\mathbf{x}, z) + \mathbf{F}^{sp}(\mathbf{x}, z) \tag{14}$$

where $\mathbf{F}^{ext}$ is an abrupt function, whereas $\mathbf{F}^{sp}$ and φ functions are smooth.

A general expression can be derived now

$$\mathbf{x}_{k+1} - (1 + H_k)\mathbf{x}_k + H_k \mathbf{x}_{k-1} = I_2 - H_k I_1 = \sum_{i=k-1}^{k+1} (S_k \mathbf{F}_k + s_k \varphi_k) \tag{15}$$

where S_k can be found from eqs.(13), and s_k are equal to

$$\begin{cases} s_{k+1} = \frac{h_k^3}{24 h_k}[G^+(2H_k^2 + H_k^3) - G^-] \\ s_{k-1} = \frac{h_{k+1}^3}{24 h_k}[-G^+ H_k + G^-(2/H_k + 1/H_k^2)] \\ s_k = \frac{h_k^2}{12}[G^+(4H_k^2 + H_k^3) + 4G^-(H_k + 1)] \end{cases} \tag{16}$$

For $G^+ = G^-$ these equations can be easily reduced to Eqs.(12).

To find $\mathbf{x}_{k+1}$, one should solve a system of non-linear equations iteratively, as earlier.

One can see, that the devised integration scheme necessitates to keep available the information about the particles dynamics in the previous steps, saving the $\mathbf{x}_{k-1}, \mathbf{x}_k, \mathbf{F}_{k-1}, \mathbf{F}_k$. Naturally, it needs an auxiliary arrays, which consume the additional memory resources. On the other hand, dealing with symmetrical beams (see above), we can save the memory capacities considerably. Namely, the opportunity to use only a part of the total symmetrical distributions allows to reduce the N_p in the model, preserving the former accuracy: for R_2 region we consider only a half of the beam and for R_3 – the quarter. Beside that, the symmetry save the mesh-arrays.

2.4 Discussion

The numerical studies have confirmed, that the proposed particle code is well adopted for beam motion simulation through HIF final objective (see below the section 3). As it was mentioned, this system must arrange a very "rigid" focusing with very big envelopes modulation. To avoid nonphysical effects, the program should operate with a large number of particles, that makes the calculations of coupled forces too time-consumed, and rapid Poisson solver, based on FFT, seems to be preferable. It is available to use 75000 particles and a spatial grid 128 x 128 in our algorithm. Beside that, the developed multistep integration scheme maintains an overall accuracy of $O(h^4)$ that radically upgrades the computational characteristics of integration block, in comparison with the second order "leap-frog" technique. The typical time of calculations for HIF final focusing objective ($\approx$ 300 steps) is about 4 hours (a personal computer PC/AT-486, supporting 4 MB memory, has been used). The usage of symmetry helps to economize the memory and does not lead to essential loss of generality.

3 Beam simulation through HIF final objective

3.1 Conventional scheme

HIF driver, which accelerates and forms the ion beams, should provide an extremely high energy deposition into the thermonuclear pellet: the total power illumination, to ensure the pellet's ignition, should be about 500 TW and the corresponding energy contribution must be 5–10 MJ (the output energy, after pellet's explosion, is expected to be about 50–150 times more, see for more details [1,2,3,4]). Such an energy can be delivered to the thermonuclear target, when using heavy ions beams, accelerated up to 10 – 20 GeV, and the current in every beam channel attains a few kA. The handling of such high-energy beams is a difficult problem by itself, when strong magnetic elements are required. Space charge forces complicate the situation by weakening the external focusing, moreover, a series of instabilities arise during the transporting through the accelerator. They can lead to rms emittance growth and deteriorate beam parameters additionally (see [13,14]).

The situation becomes even more difficult in the driver's final stage, when beam current attains its maximum and ion focusing onto the small thermonuclear target occurs — very strong quadrupole lenses with big apertures must be taken. The typical magnifying coefficient $\lambda \approx 100$ where $\lambda = g_{max}/g_{min}$ (g stands for the beam's sizes). Such a large envelopes modulations occur within a fairly short distance (8-10 meters), and, as it was mentioned above, the situation becomes very sensitive to beam current variations and ions momenta spread.

Let us consider the ion beam Bi^{+2} with energy 20 GeV, the emittances $\epsilon_x = \epsilon_y = 4.5\pi cm \cdot mrad$ and the beam current 2.25 kA, which should be focused onto the thermonuclear pellet with radius r=3 mm. In the paper [16] a

quadrupole focusing objective was designed. The optical parameters of the objective were found by the fitting algorithm, in frames of K-V equations and fig.5 demonstrates the beam envelopes through the objective. As it was found, the pole-tip fields attain a few (5-6) Tesla, that necessitates to use the superconducting lenses and the magnifying coefficient $\lambda = 90$. In the paper [16] beam losses, due to ion bunches longitudinal non uniformity, were minimized and it was found, that the non symmetrical focusing regime ($x_{max} \times y_{max} = 3.0 \times 2.5\ mm^2$) at the target may reduce the losses due to momenta dispersion.

The designed final focusing system has been studied by particle simulation, when ion beam has a microcanonical K-V distribution at the entrance of the objective. As it was mentioned above, the density of K-V beam has uniform projections and a sharp edge at the beam's boundary. Since the finite-sized particles are used in the particle code, this edge will be diluted and the corresponding density - smoothened, that will contribute nonlinear terms in the space charge field (see for example figs.4a - 4b). Beside that, K-V equations are valid only in a free space, whereas our 2D code operates within finite space region (that seems to be more practical). Particle simulation, therefore, must produce the result, which will differ from the K-V equations integration.

Meantime, computer modeling by our code has demonstrated, that beam sizes are close to the idealized envelope model, as it has been plotted in fig.5. At the target (S_T=37.1 m) the difference from the ideal focusing becomes more significant, but, not critical still. Namely, we have: $x_{max} \times y_{max} = 3.06 \times 3.4\ mm^2$ and $(< x^2 >< y^2 >)^{1/2} = 1.47 \times 1.7\ mm^2$ (correspondingly $3 \times 3\ mm^2$ and $1.5 \times 1.5\ mm^2$ for ideal model); the rms emittance growth is practically absent ($|\Delta\varepsilon_{x,y}/\varepsilon_{x,y}| \leq 0.5\%$), that indicates a good coincidence with the singular K-V equations. The ions coordinates at the target (in phase-space and in real space) shows the good enough quality of the focusing (see figs.6a –6c. The ions losses are about 8.9%. (Since the longitudinal density is not uniform, the total losses will be more. To take into account this circumstance, however, a more advanced 3D code must be used).

Fig.7 shows the real space density of beam with water-bag phase density at the objective entrance. Again, beam behavior is similar to that, which is plotted in the fig.5. Fig.8a shows the rms emittance growth due to the nonlinear space charge forces: $|\Delta\varepsilon_{x,y}/\varepsilon_{x,y}| \leq 25\%$. The ions coordinates at the target, plotted in figs.8b - 8d, indicate the dilution of focusing spot at the target. The total ion losses grow up to 20%.

In the above described parameters of HIF driver it has been assumed, that the target illumination must be symmetric. Strictly saying a spherically symmetric beam focusing in the thermonuclear reactor chamber must be arranged (up to 24 beam channels should be constructed); beside that, the ion bunches must be thoroughly synchronized (pulse duration is $\approx$ 15–20 ns) to ensure a uniform illumination of a pellet. It's clear, that this sophisticated scheme can scarcely be realized in practice. More realistic way is to use the so-called "indirect target", when the thermonuclear pellet ablates by X-ray radiation, induced

by the heavy ion beam (see reference [17]). However, the specific power deposition required to ignite this target, should be of the order 10^{16} W/g, that necessitates to increase beam current magnitude significantly.

At the same time, during the numerical experiments, we could see, that the further beam current growth in frames of the designed focusing objective, can be hardly realized: too big ion losses occur at the target, as well as very strong focusing lenses, with big apertures, are to be used. Thus, the indirect target demand a serious reconsideration of the driver's concept.

3.2 Charge-symmetrical scheme

Recently a new idea has been reported (see ref. [18]) to suppress the space charge effects by use of beams with equal currents of negative and positive ions. In the capacity of the accelerated ions, some heavy metals, may be chosen, which give stable enough negative ions. Notice, that the neutralization should be combined with the use of a family of negative and positive ions with different masses (isotopes), that permits to upgrade the accumulated energy of ions. We omit, however, these effect, assuming the beam current is constant. In the paper [18] the optimal choice of ions was discussed (four platinum isotopes should be used), and the following driver's parameters were declared: total energy is 9 MJ, total power illumination is 600 TW, ions energy is 10 GeV, specific power deposition is 10^{16} W/g, that will ensure a reliable ignition of the target.

One can see, that the ideal neutralization is valid, when positive and negative ion beams have the same sizes. If these beams differ from each other, then the nonlinear forces arise and when using quadrupole (alternative-gradients) focusing, the influence of nonlinearities becomes inevitable. At the same time, during beam propagation through the long periodical focusing channel, one can reduce these effects essentially, by decreasing the focusing channel's phase advance (see figs.9a – 9b). The corresponding envelopes modulation will be decreased as well, and, as a result, space charge influence will be suppressed. Taking, for example, $\mu = 40°$, we obtain quasi-symmetrical quasi-neutralized beam, whereas on choosing $\mu = 80°$, the difference between the positive and negative envelopes will contribute the undesirable non-linear components in the space charge field.

As regards to final focusing objective, the beam dynamics, as we could see above, must be non symmetrical. The nonlinear Coulomb effects, therefore, will arise and deteriorate the focusing. We try, however to control the influence of these effects, taking into account the above considerations. In the figure 10 one can see a zero-current beam through the final focusing system. The periodical channel, which precedes the final objective, has phase advance $\mu_0 = 40°$. Platinum ions have been considered (see reference [18] for more details). The optical lattice has been designed by means of matching algorithm from [16]. Then, a numerical experiment has been implemented by our 2D particle code on beams dynamics with beam currents $I = 5$ kA for each component of the

beams (the total current will attain, obviously, 10 kA) (see fig.11a).

One can see, that the envelopes behavior remains similar to zero-current beam motion, whereas the conducting such a significant ion currents through the final focusing system without space charge compensation would necessitate unattainable strong focusing lenses with very big apertures, that seems practically unrealizable. On leaving the channel, a quasi-adiabatic beam behavior is being maintained up to $s = 60$ m, when rms emittances growth $|\Delta\varepsilon_{x,y}/\varepsilon_{x,y}|$ is absent. However, within a short interval $60 < s < 75$ m, we observe emittance's blow-up, due to nonlinear space charge forces (see fig.11b). We can see ion's phase coordinates (x, x') and projections into real space (x, y) at thermonuclear target (see figs.12a – 12d). The total ions losses are 47%.

As regards to computational aspects, we notice, that during calculations we have varied the longitudinal step of integration h, when ion's trajectories change slowly (see fig.11a). Namely, it has appeared to be helpful to increase h within the drift space interval $(20 \leq s \leq 60$ m) and to decrease h magnitude, when beam modulations are significant $(60 \leq s \leq 70$ m). This opportunity speeds up the calculation and does not violate the accuracy.

Thus, after the preliminary numerical studies, we could see, that the neutralization allows to conduct very intense beams through the periodical transport channel without essential growth of effective phase volume, whereas a serious beam parameters deterioration occurs within a very short distance in the final objective. Hence, a further optimization of final focusing should be performed, in order to reduce the ions losses at the thermonuclear target. After that an universal 3D particle simulation, which takes into consideration all longitudinal effects must be performed.

Acknowledgements

The author is indebted to Prof. P.R. Zenkevich for scientific guidance and useful comments and wish to thank Prof. D.G. Koshkarev for his interest to this work.

Appendix 1

To find the distribution $\{H_i\}$, one should solve the following non-linear programming problem:

$$\Phi(\delta_1,\ldots,\delta_{m-1}) = \sum_{i=1}^{m-1}\left\{\int_{H_i}^{H_i+\delta_i} f(H)HdH - \frac{1}{n}\int_{H_1}^{H_m} f(H)HdH\right\}^2 \xrightarrow{\vec{\delta}} \min$$

subject to

$$\sum_{i=1}^{m-1}\delta_i = H_m$$

where $\delta_i = H_{i+1} - H_i$.

The numerical procedure to find $\vec{\delta}$ (and hence, the distribution $\{H_i\}$) is described in [9] in detail.

Appendix 2

According to Simpson's formula, an approximate value I_1 of the integral $\mathcal{I}_1$ can be calculated, using $\mathbf{F}(z_{k-1})$, $\mathbf{F}(z_k)$, $\mathbf{F}(z_{k+1})$ valnes:

$$I_1 = \frac{h_k}{6}\{0 + 4(z_{k-1} - z_{k-1/2})\mathbf{F}_{k-1/2} + (z_{k-1} - z_k)\mathbf{F}_k\}$$

Since $z_{k-1} - z_{k-1/2} = -h_k/2,\ z_{k-1} - z_k = -h_k$, we obtain

$$I_1 = -\frac{h_k^2}{6}\{2\mathbf{F}_{k-1/2} + \mathbf{F}_k\}. \tag{17}$$

Ana logically, I_2 can be calculated from

$$I_2 = +\frac{h_{k+1}^2}{6}\{2\mathbf{F}_{k+1/2} + \mathbf{F}_k\}. \tag{18}$$

The following expansions can be written

$$\begin{cases} \mathbf{F}_{k+1/2} = \mathbf{F}_k + \mathbf{F}'_k h_{k+1}/2 + \mathbf{F}''_k(h_{k+1}/2)^2/2 + \delta_{k+1}h_{k+1} \\ \mathbf{F}_{k-1/2} = \mathbf{F}_k - \mathbf{F}'_k h_k/2 + \mathbf{F}''_k(h_k/2)^2/2 - \delta_k h_k \end{cases} \tag{19}$$

where $\delta_{k+1} = \mathbf{F}_k^{(3)}(\xi_{k+1})h_{k+1}^2/6$, $\delta_k = \mathbf{F}_k^{(3)}(\xi_k)h_k^2/6$, and

$$\mathbf{F}'_k = \mathbf{F}_{k+1}\frac{h_k}{2h_{k+1}\hat{h}_k} + \mathbf{F}_k\{\frac{1}{h_k} - \frac{1}{h_{k+1}}\} - \mathbf{F}_{k-1}\frac{h_{k+1}}{2h_k\hat{h}_k} + O(\hat{h}_k^2)$$

$$\mathbf{F}''_k = \mathbf{F}_{k+1}\frac{1}{h_{k+1}\hat{h}_k} - \mathbf{F}_k\{\frac{2}{h_{k+1}h_k} + +\mathbf{F}_{k-1}\frac{1}{h_k\hat{h}_k} + O(\hat{h}_k^2)$$

Finally, substituting the expressions (19) in (17)-(18), we obtain the scheme (12).

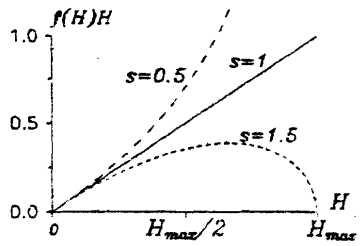

Fig. 1a

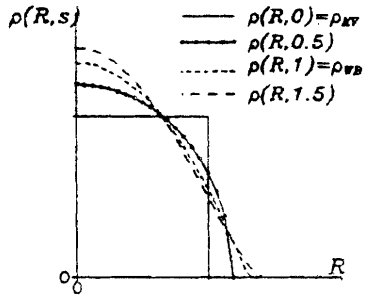

Fig. 1b

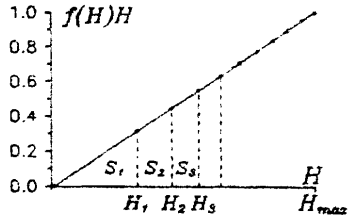

Fig. 1c

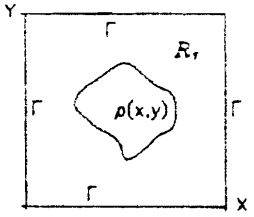

Fig 2a

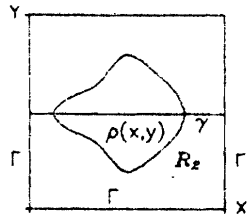

Fig. 2b

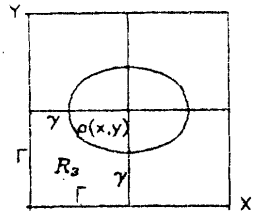

Fig. 2c

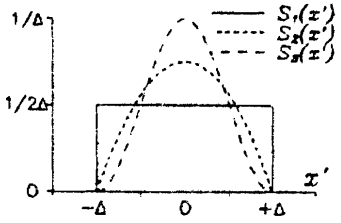

Fig. 3c

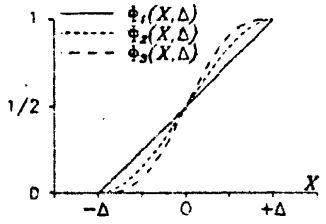

Fig. 3b

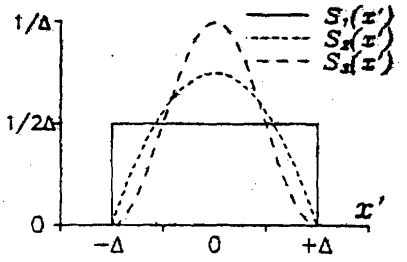

Fig. 3a

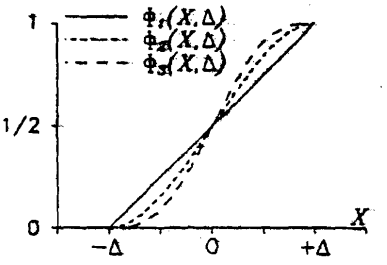

Fig. 3b

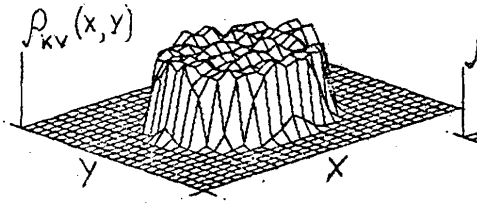

Fig. 4a

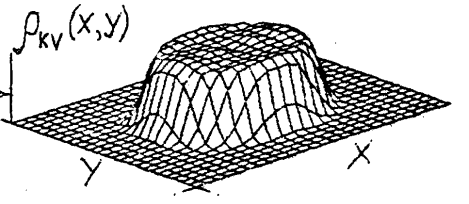

Fig. 4b

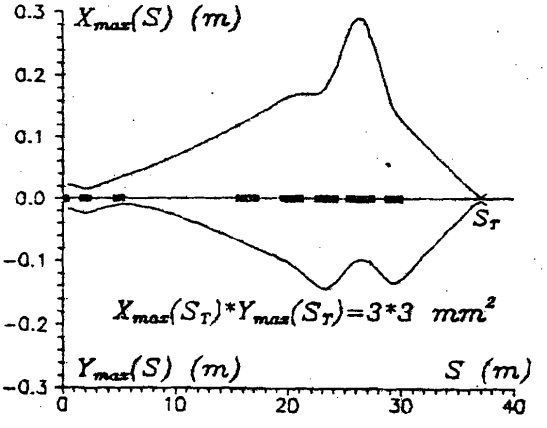

Fig. 5

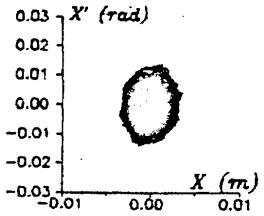

Fig. 6a

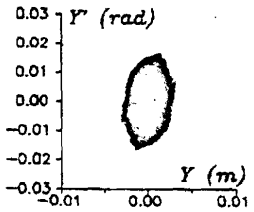

Fig. 6b

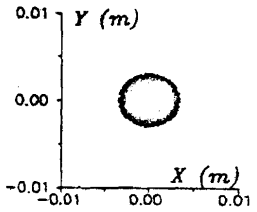

Fig. 6c

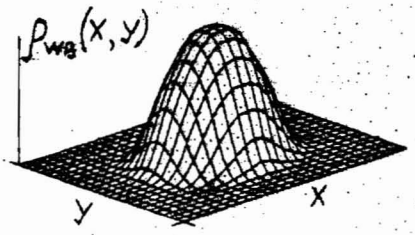

Fig. 7

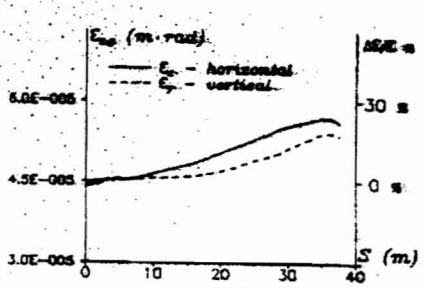

Fig. 8a

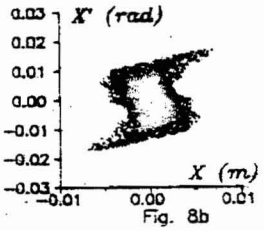

Fig. 8b

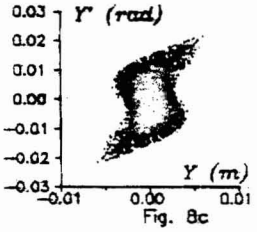

Fig. 8c

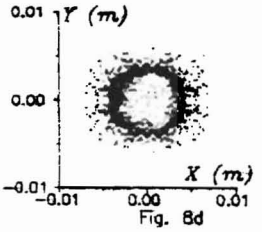

Fig. 8d

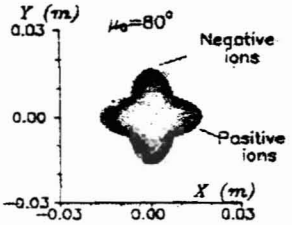

Fig. 9a

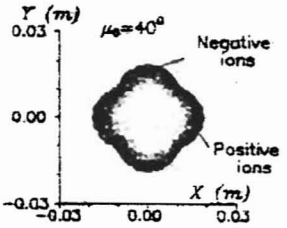

Fig. 9b

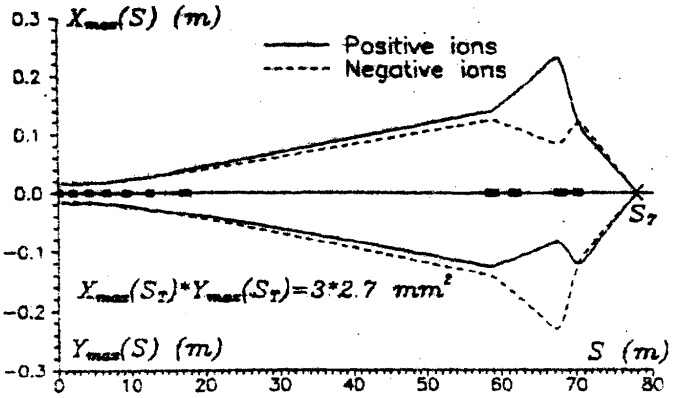

Fig. 10

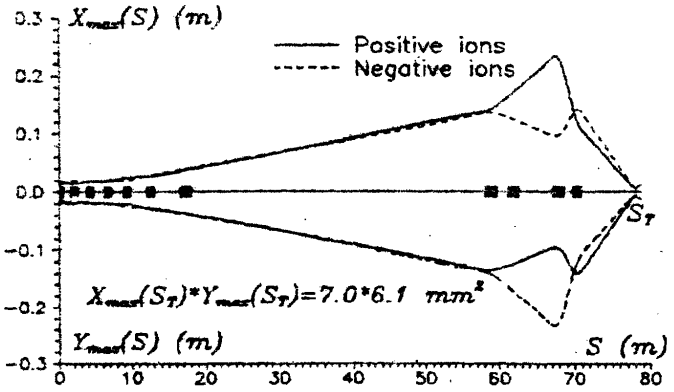

Fig. 11a

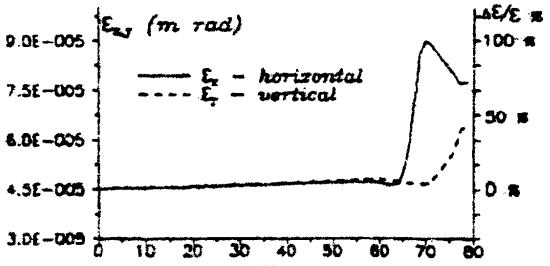

Fig. 11b

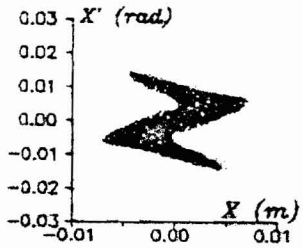

Fig. 12a

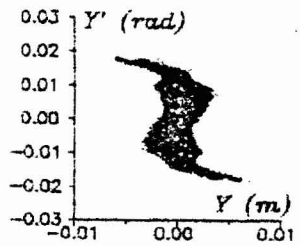

Fig. 12b

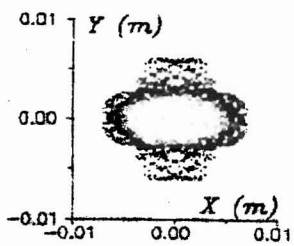

Fig. 12c

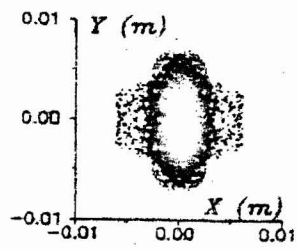

Fig. 12d

Figure 1: (a) $f(H)H$ for $s = 0.5$, $s = 1.0$ and $s = 1.5$, (b) $\varrho(x,y)$ for $s = 0.5$, $s = 1.0$ and $s = 1.5$, (c) $\{H_i\}$ and $\{S_i\}$ for $F(H) \equiv 1$.

Figure 2: Space charge density $\varrho(x,y,0)$ for (a) general case, (b) double symmetry, (c) quadruple symmetry.

Figure 3: a) Shape functions $S(x')$, b) $\int_{-\Delta}^{x} S(x')dx'$.

Figure 4: Space charge density $\varrho(x,y,z)$ (KV-distribution) for various forms of particle's cloud a) NGP-method, b) Shape function is $S_3(x')$.

Figure 5: KV-beam motion through final focusing objective (envelope equations model).

Figure 6: Ions coordinates at the target: (a) (x,x'), (b) (y,y'), (c) (x,y).

Figure 7: Space charge density $\varrho(x,y,z)$ for WB-distribution (shape function is $S_3(x')$).

Figure 8: (a) RMS emittances through final focusing objective (WB initial distribution), ions coordinates at the target: (b) (x,x'), (c) (y,y'), (d) (x,y).

Figure 9: Ions coordinates for charge-symmetrical beam in periodical channel: (a) $\mu = 80°$, (b) $\mu = 40°$.

Figure 10: Zero-current beam through final focusing objective ($\mu = 40°$ in the regular transport channel).

Figure 11: (a) High-current beam $I = 5kA$ through the final focusing system, (b) Corresponding RMS emittances within the focusing system (for negative beam solid line will correspond to ε_y and the dash line — to ε_x.

Figure 12: Ions coordinates at the thermonuclear target: (a) (x,x'), (b) (y,y') (for negative ions – visa versa), (c) (x,y) for positive ions, (d) (x,y) for negative ions.

References

[1] Proc. of HIF Workshop, Brookhaven National Laboratory, 1977, BNL-50769.

[2] Proc. of HIF Workshop, Argonne National Laboratory, 1978, ANL-79-41.

[3] Proc. of HIF Workshop, Berkeley, California, 1979, LBL-10301.

[4] "HIBALL-II An Improved Conceptual Heavy Ion Beam Driven Fusion Reactor Study", KfK 3840, FPA-84-4, UWFDM-625, Kernforschungszentrum, Karlsruhe, 1985.

[5] I.M.Kapchinskij and V.V.Vladimirskij, Proc. Inter. Conf. on High Energy Accelerators, CERN, Geneva, 1959, p.274.

[6] J.D.Lawson "High current beam transport", Proc. of the 1984 Linear Acc. Conf., FRG, GSI-84-11, p.298.

[7] F.J.Sacherer "RMS envelope equations with space charge", IEEE Trans. Nucl. Sci., NS-18, 1971.

[8] R.W.Hockney "Computer simulation using particles", McGraw-Hill Inc., 1981.

[9] L.G.Vorobiev, Dissertation, ITEP, Moscow, 1991.

[10] H.Abe et al. "Grid Effects on the Plasma Simulation", J. Comput. Phys., vol. 19, pp.134-149.

[11] L.G.Vorobiev, "Rapid Poisson solver, based on Fast Fourier Transformation for bivariate regions with various boundary conditions", Preprint ITEP-193, 1984, Moscow.

[12] L.G.Vorobiev, "Fourth-order scheme for high current beam motion equation integration", Preprint ITEP-38, 1988, Moscow.

[13] I.Hofmann et al. "Stability of Kapchinskij-Vladimirskij (K-V) Distribution in long periodic transport systems" Particle Accelerators, 1983, Vol. 13, pp.145-178.

[14] J.Struckmeier, J.Klabunde, M.Reiser "On the stability and emittance growth of different particle phase-space distributions in a long magnetic quadrupole channel", Particle Accelerators, 1984, Vol.15, pp. 47-65.

[15] A.Garren "Studies of a beam for transport to a target", Proc. HIF Workshop, Argonne National Laboratory, ANL-79-41, pp. 397-402.

[16] L.G.Vorobiev, P.R.Zenkevich, D.G.Koshkarev, Atomnaya Energiya, vol.63, No.3, 1987, pp.202-206.

[17] R.C. Arnold and R.W. Müller "Heavy-ion driver concept for laboratory implosion experiments", GSI-90-15 Report, Oct. 1990, Darmstadt, Germany, p.37.

[13] D.G.Koshkarev "Charge-symmetrical driver for heavy ion fusion", Preprint ITEP-7, 1994, Moscow.

Л.Г.Воробьев
Два Д код для моделирования пучка в драйвере для ИТИС.

Подписано к печати 01.03.94 Формат 60x90 1/16 Офсетн.печ.
Усл.печ.л.1,5 Уч.-изд.л. 1,1 Тираж 94 экз. Заказ 22
Индекс 3649

Отпечатано в ИТЭФ, 117259, Москва, Б.Черемушкинская,25